

CHAPTER III. QUANTITATIVE EFFECT OF SCAFFOLD ABUNDANCE ON SIGNAL PROPAGATION

1. Abstract

Protein scaffolds bring together multiple components of a signaling pathway, thereby promoting signal propagation along a common physical “backbone.” Scaffolds play a prominent role in natural signaling pathways and are emerging as a promising platform for synthetic circuits. To better understand how scaffolding quantitatively affects signal transmission, we conducted an *in vivo* experimental sensitivity analysis of the yeast mating pathway to a broad range of perturbations in Ste5 abundance. Our results demonstrate that the expression level of Ste5 significantly affects several quantitative aspects of signal propagation, including signal throughput, pathway ultrasensitivity and baseline leakage. Some of these effects, such as changes in pathway responsiveness to pheromone stimulation, impact the ultimate physiological response of yeast cells. In contrast, other effects, such as the baseline leakage in MAP kinase signaling at higher expression levels of Ste5, remain buffered and do not propagate downstream. Our quantitative measurements reveal performance tradeoffs in scaffold-based modules and help to define engineering challenges for implementing molecular scaffolds in synthetic regulatory versus metabolic pathways.

2. Introduction

Protein scaffolds bind concomitantly to multiple components of a signaling pathway, thereby organizing signal transmission onto a common physical backbone (Bhattacharyya et al., 2006b). Scaffold-based modules are broadly used to propagate signals that regulate cell cycle, proliferation, differentiation and motility in species ranging from yeast to human (Pawson and Scott, 1997). Scaffolds are also emerging as a promising platform for engineering synthetic signaling modules. Molecular redesign of scaffolds has been used to alter the repertoire of scaffold binding partners, thereby redirecting signal flow (Park et al., 2003) and altering signal dynamics (Bashor et al., 2008).

In addition to the molecular design of the scaffold, the quantitative performance of scaffold-based modules will depend on the expression level of the scaffold and its binding partners. Computational models have been used to examine how the expression levels of module constituents may contribute to signal throughput (Levchenko et al., 2000). These models predict that scaffolds may not always promote signal propagation. When scaffold concentration exceeds an optimal level, enzymes and substrates are predicted to bind to distinct scaffolds rather than onto a single backbone, thereby inhibiting signal transmission via combinatorial inhibition.

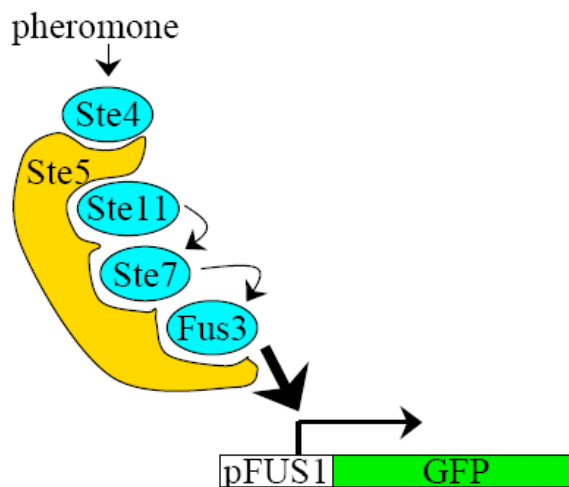


Figure III-1. The Ste5 scaffold and the pheromone MAP kinase pathway in *S. cerevisiae*.

Ste5 has independent binding sites for Ste4, Ste11, Ste7 and the MAP kinase, Fus3. Another MAP kinase, Kss1 (not depicted for clarity), also binds Ste5, albeit with lower affinity than Fus3, and is also activated by Ste7. Upon pheromone stimulation, Ste5 facilitates signal transmission from Ste4 to Fus3/Kss1. Active Fus3 and Kss1 trigger the transcription of *FUS1*, cell cycle arrest, and ultimately mating.

These and other model predictions, however, are based on idealized mathematical representations of scaffold-based signaling. In contrast, scaffold-mediated signaling *in vivo* is often far more intricate as exemplified for the prototypical scaffold Ste5 in yeast cells (Figure III-1). Some of the binding partners of Ste5 (e.g., Ste7 and Fus3) dock with each other independent of the scaffold (Bardwell et al., 1996). This scaffold-independent interaction may compete with scaffold-mediated signaling, rendering scaffold-based signaling ‘brittle’ to variations in the expression levels of critical components (Ferrell 2000). Furthermore, dimerization of Ste5 and other scaffolds is a critical step in signal transmission (Yablonski et al., 1996) and may contribute to apparent cooperativity

(Ferrell 2000). In addition, Ste5 translocates between different subcellular compartments (Pryciak and Huntress, 1998; van Drogen et al., 2001), is regulated by Fus3-mediated negative feedback (Bhattacharyya et al., 2006a) and binds competitively to multiple proteins (Fus3 and Kss1) with different affinities (Kusari et al., 2004). This complex array of mechanisms conceals precisely how real scaffolds such as Ste5 quantitatively contribute to signal transmission *in vivo*.

To better understand the quantitative contribution of the Ste5 scaffold to signal transmission, we conducted an *in vivo* experimental sensitivity analysis of the mating pathway to a broad range of perturbations in Ste5 abundance. Our results demonstrate that perturbations in scaffold abundance have significant effects on several quantitative aspects of signal propagation, including signal throughput, baseline drift and pathway ultrasensitivity.

3. Results and Discussion

3.1 Modulation of scaffold expression level

To better understand the quantitative effect of scaffold abundance on pheromone-mediated MAP kinase signaling, we engineered a panel of yeast strains that express Ste5 at different levels. Starting with a *ste5Δ* null parent strain, we introduced a C-terminal, myc-tagged version of *STE5* under the regulation of various constitutive promoters (Mumberg et al., 1995) and measured the relative expression level of Ste5 in the different strains by a quantitative immunoblot procedure (see Materials and Methods and Figure III-8 in Supplementary Data). Ste5 expression in this panel of yeast strains spanned nearly two orders of magnitude (Figure III-2). The highest level of expression was 50-fold greater than that supported by the wild-type *STE5* promoter.

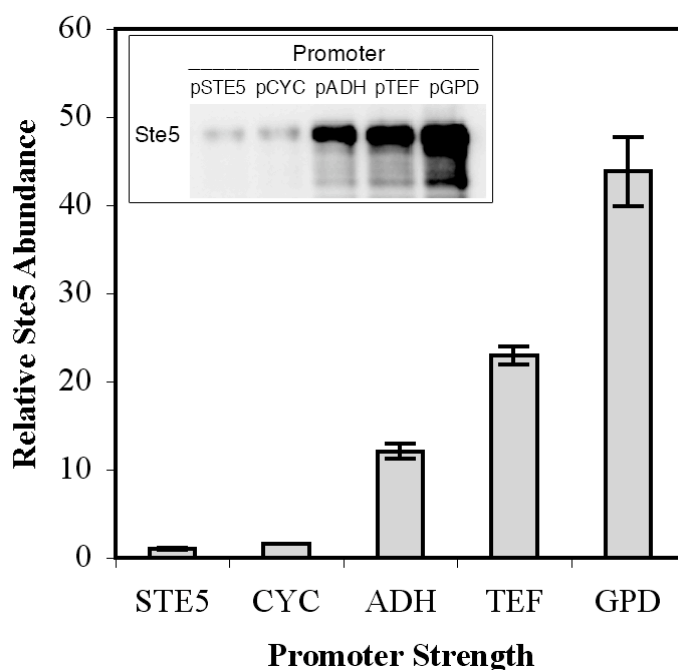


Figure III-2. Modulating the expression level of the scaffold Ste5.

Myc-tagged Ste5 was expressed behind an array of constitutive promoters (pCYC, pADH, pTEF and pGPD), including the wild-type *STE5* promoter (pSTE5). Vectors were transformed into a *ste5Δ* yeast strain, and the relative expression levels of Ste5 were measured by quantitative immunoblot with standard curve. Error bars denote standard error (n=3).

3.2 Effect of scaffold on signal throughput and pathway ultrasensitivity

To quantify the sensitivity of the mating pathway to Ste5 abundance, we measured the mating transcriptional response over a broad range of α -factor concentrations in our panel of yeast strains. Variations in scaffold abundance had a significant effect on the transcriptional output of the mating pathway (Figure III-3). At every dose of the α -factor stimulus, the output was biphasic with respect to the level of Ste5, revealing that an optimum level of Ste5 scaffold is needed to maximize signal throughput. This biphasic relationship is consistent with model predictions (Levchenko et al., 2000) and with previous studies of mammalian scaffolds JIP and KSR (Ferrell, 2000; Levchenko et al., 2000). Past studies involving Ste5 overexpression reported only signal augmentation (Kranz et al., 1994) (Choi et al., 1994; Kranz et al., 1994). Our data shows, however, that this may have been a limitation in the range of Ste5 overexpression explored in those studies rather than a fundamental difference between Ste5 and mammalian scaffolds.

(Section 3.2 continues after Figure III-3.)

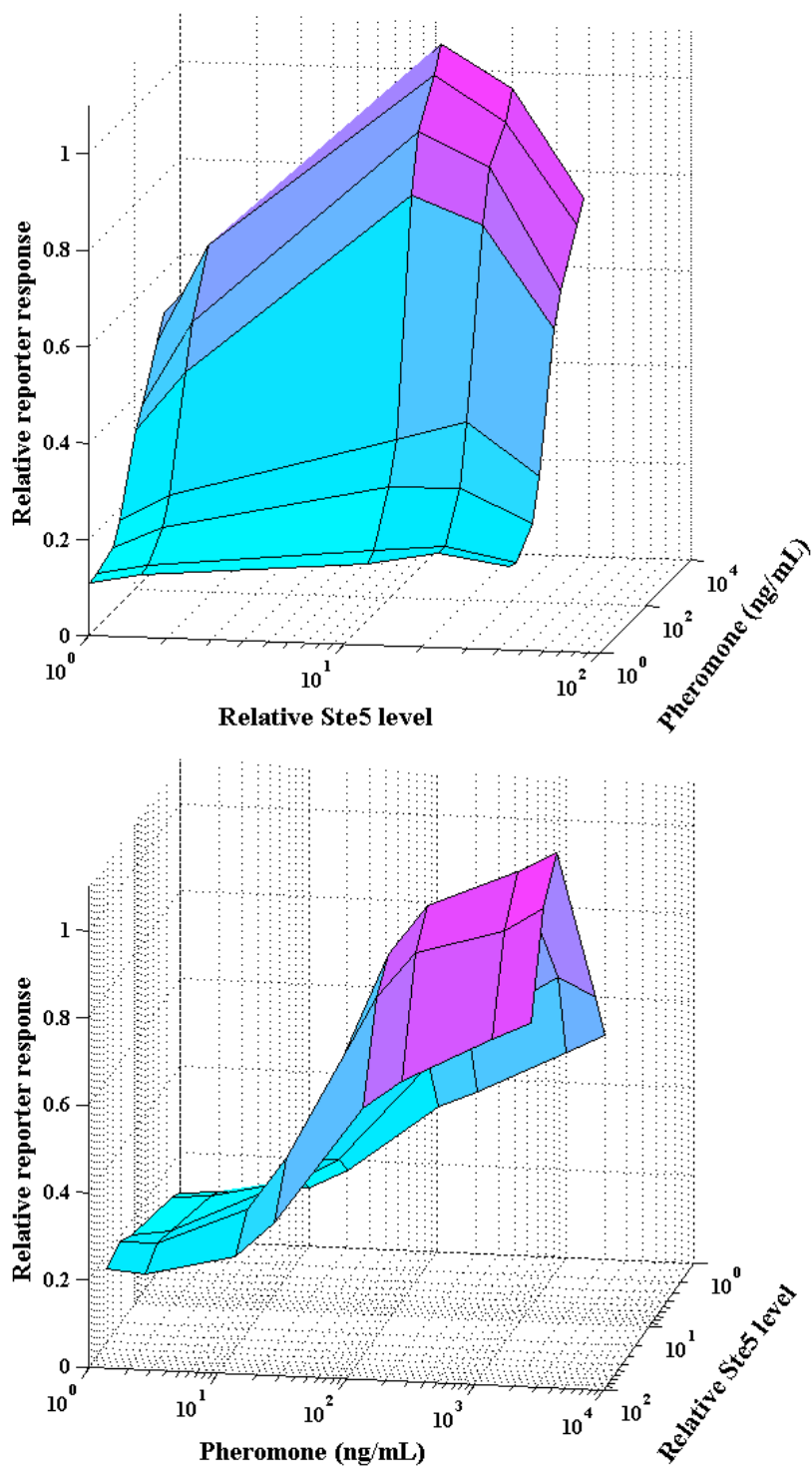


Figure III-3. Sensitivity analysis of mating pathway response to perturbation in scaffold abundance.

Yeast cells expressing different levels of Ste5 were induced with α -factor for 2.5 h. The pFUS1-GFP reporter response was measured by flow cytometry. The relative mean GFP fluorescence is shown for the various Ste5 expression levels and α -factor doses. Two different views of the surface plot are shown.

In addition to the magnitude of pathway response, Ste5 abundance has a significant effect on the responsiveness of the mating pathway. Fitting the Hill equation to the dose-response curves revealed that both the Hill coefficient (n_H) and the pheromone dose at which half-maximal response is achieved ($EC50_\alpha$, a widely used biological metric that is inversely related to stimulus potency) are significantly affected by Ste5 expression level (See Supplementary Data, Figure III-9, and Table III-3). At the wild-type level of Ste5, approximately a greater than 100-fold change in pheromone concentration was required to shift from 10% to 90% of maximal response ($n_H = 0.93$); in contrast, at the optimum dose of Ste5, a 25-fold change in pheromone concentration was sufficient to achieve an equivalent shift in reporter output ($n_H = 1.4$). This enhanced cooperativity did not involve a shift from graded to all-or-none response at the single-cell level (Figure III-9). Rather, at the optimum scaffold expression level, the transcriptional output in individual cells was more responsive to changes in pheromone concentration. In addition to a steeper response to pheromone dose, the $EC50_\alpha$ shifted from 100 ng/mL to 50 ng/mL when Ste5 expression is increased from its wild-type level to its optimum.

These measurements reveal that maximum signal throughput, apparent cooperativity and α -factor potency occur at approximately the same optimum level of Ste5. To test whether these significant changes in the transcriptional response translate to the ultimate biological response, we assessed the mating response of yeast cells using the halo assay. Here, the pheromone is supplied from a central source and induces cell cycle arrest up to a radius beyond which the pheromone concentration is too low for cells to respond. Since the $EC50_\alpha$ of the transcriptional response is sensitive to Ste5 level, we

tested whether the radius of the halo exhibits a similar dependence on scaffold expression level. As Ste5 expression was increased from its wild-type level, the size of the mating halo increased until reaching a maximum at an optimal dose of Ste5 (Figure III-4). Increasing Ste5 expression level beyond this optimum reduced the size of the mating halo. The optimum level of Ste5 that maximizes the halo radius precisely correlates with the optimum Ste5 level for transcriptional response.

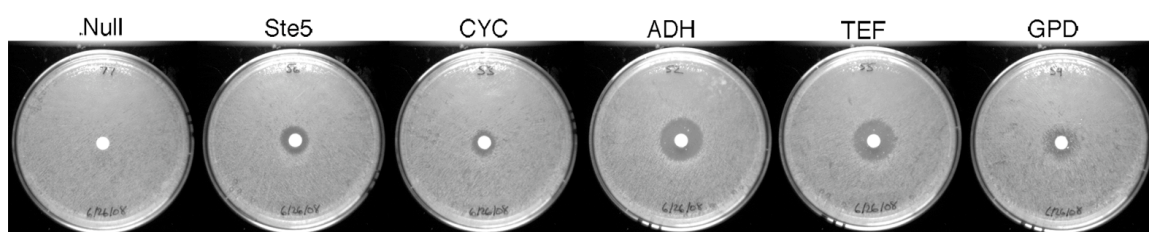


Figure III-4. Perturbation of scaffold abundance quantitatively alters phenotypic response.

The mating halo assay was performed in cells expressing different levels of Ste5. Results from a single representative out of two independent trials are shown.

3.3 Closer examination of the Ste5 module

Transcriptional response and cell-cycle arrest are several steps downstream of the direct MAP kinase outputs of the Ste5 scaffold. To confirm that the effect of Ste5 perturbations on the mating pathway truly emanates from the direct outputs of the Ste5 module, we measured the phosphorylation of the mating MAP kinases, Fus3 and Kss1, by quantitative Western blotting. At the saturating dose of 2 $\mu\text{g/mL}$ α -factor, the levels of both phospho-Fus3 and phospho-Kss1 exhibit a biphasic dependence on Ste5 abundance (Figure III-5). Furthermore, the biphasic dependence of MAP kinase signaling on

scaffold abundance closely matches the trend in the transcriptional output (Figure III-6).

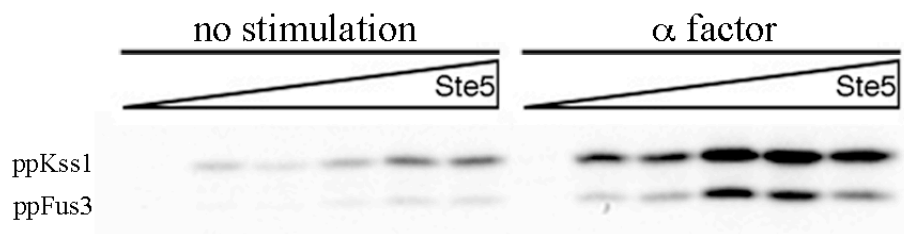


Figure III-5. Phospho-MAPK response to perturbation in Ste5 expression.

Yeast cells were induced with α -factor or left unstimulated for 15 minutes and phospho-Fus3 and phospho-Kss1 were analyzed by immunoblot.

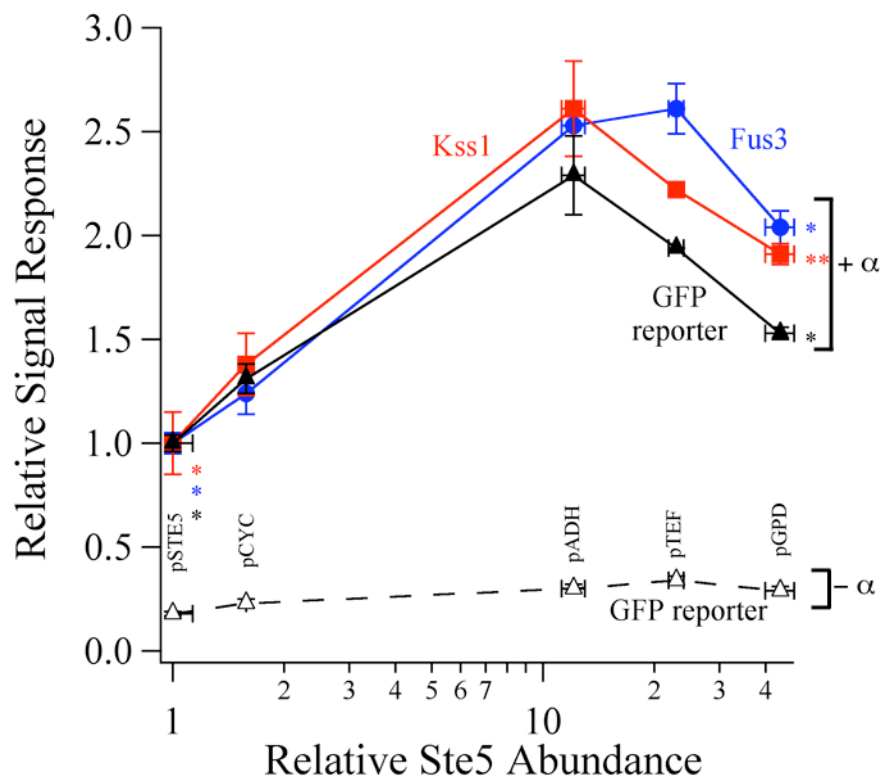


Figure III-6. Quantitative measurements of phospho-MAP kinase and pFUS1-GFP responses.

The levels of the phospho-MAP kinases were normalized by their respective total protein expression. Error bars denote standard error ($n=3$). The *asterisks* indicate the p -value between the marked data point and the maximum data point for a given curve: *, $p < 0.01$ and **, $p < 0.05$ (Student's t test).

These measurements also revealed that both phospho-Fus3 and phospho-Kss1 exhibit a similar biphasic dependence on Ste5 abundance, suggesting that a common upstream factor, such as Ste7, may be the limiting component. To test this hypothesis, we overexpressed HA-tagged Ste7 in our panel of yeast strains that express Ste5 at different levels (Figure III-7). In parallel, we constructed a control panel of yeast strains that carries an empty control vector. At low scaffold abundance, overexpression of Ste7 did not appreciably alter the mating reporter response relative to control cells carrying the empty vector (Figure III-7). However, at higher scaffold concentrations, overexpression of Ste7 significantly increased the reporter response and eliminated the downturn in signal throughput.

These results demonstrate a scaffold-limited and Ste7-limited regime of signaling. When the scaffold is the limiting factor to signal throughput (for scaffold doses below the optimum), increasing the expression of Ste7 had no effect on signal throughput. However, past the optimum dose of scaffold, signal throughput was limited by Ste7. Overexpression of Ste7 eliminated the biphasic dependence of signal throughput on scaffold amount, at least within the range of Ste5 expression explored. We reason that the optimum Ste5 dose has shifted to a level higher than that captured by our panel of yeast strains. These results demonstrate quantitatively that the abundance of scaffold and its binding partners together shape the biphasic dependence of signal throughput and determine the optimum dose of scaffold.

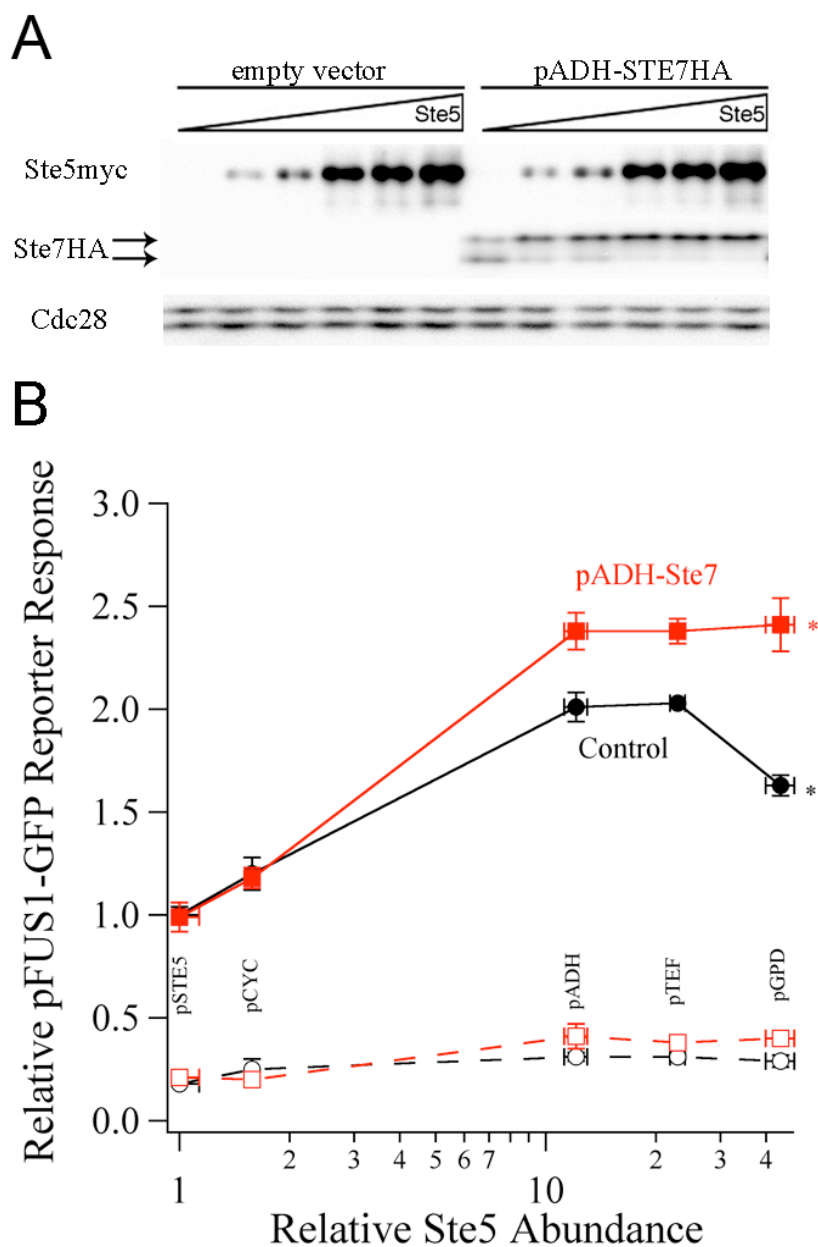


Figure III-7. Scaffold-limited and Ste7-limited regimes of signaling.

(A) Yeast strains expressing different levels of Ste5 were transformed with either an empty vector control or a vector encoding HA-tagged Ste7 downstream of an ADH promoter. The expression of Ste5myc and Ste7HA were confirmed by immunoblot. (B) Yeast overexpressing Ste7 or not were stimulated with α -factor for 2.5 h, and the pFUS1-GFP reporter response was quantified by flow cytometry. Error bars denote standard error (n=4). The *asterisks* indicate the *p*-value between the marked data points: *, $p < 0.01$ (Student's *t* test).

3.4 Sensitivity of signal quality to scaffold abundance

Our data demonstrate that the optimum dose of Ste5 provides a number of improvements to signal transmission and raises the question of whether there are tradeoffs in other metrics of pathway performance. Scaffolds play an important role in maintaining the fidelity of stimulus-response relationships between pathways that use a common pool of signaling intermediates. We tested whether changes in Ste5 expression level affect cross-activation between two closely related pathways, the pheromone and the high-osmolarity MAP kinases pathways (see Supplementary Data and Figure III-10). Pheromone stimulation activated only the mating MAP kinases and did not stimulate phosphorylation of Hog1, the high-osmolarity MAP kinase. Meanwhile, stimulation with sorbitol appropriately activated Hog1 with no cross-activation into the pheromone pathway. Thus, across nearly 50-fold change in Ste5 expression level, signal fidelity is maintained.

Another important metric of the performance of signaling modules is the signal-to-noise ratio. High-quality signal transmission involves maintaining a low baseline signal in the absence of stimulation, while responding with a strong signal when the stimulus is present. To investigate the effect of increased scaffold abundance on baseline signaling, we examined the phosphorylation of Fus3 and Kss1 in the absence of pheromone. Our measurements show that increasing Ste5 expression elevates the basal activities of Fus3 and Kss1 (Figure III-5). In fact, the baseline level of phosphorylated Fus3/Kss1 among cells expressing high levels of scaffold was equal to the pheromone-induced response in cells expressing wild-type levels of Ste5. Interestingly, this

significant baseline leakage in Fus3/Kss1 signaling is not propagated to the downstream transcriptional response. The baseline pFUS1-GFP response exhibited little change across a 50-fold change in Ste5 expression (Figure III-6). Thus, although baseline activation of the immediate outputs of the Ste5 module is compromised, the downstream transcriptional mating response is buffered and maintains a normal baseline level at all expression levels of Ste5.

3.5 Potential implications for natural and synthetic scaffold-based modules

Our results reveal that the wild-type expression level of Ste5 is not set for optimum throughput and responsiveness (Figure III-3) and suggest potential reasons for this sub-optimal configuration. The most straightforward explanation is that operating at half-maximal throughput permits regulatory flexibility to tune up or down module performance. Indeed, our data show that such modulation of throughput would have quantitative effects on the ultimate biological response. Furthermore, operating in the Ste5-limited regime permits the tuning of pathway performance solely by tuning altering Ste5 expression level and makes the module less sensitive to perturbations in other module components. Finally, our measurements suggest that there may be a penalty for operating at the optimum level of Ste5. Baseline activation of Fus3/Kss1 significantly increases; while this baseline leakage does not affect the quality of the mating response, other cellular activities regulated by these kinases may be adversely affected.

Molecular scaffolds offer a promising platform for engineering synthetic regulatory and metabolic circuits. Our results suggest that baseline leakage may be a

potential design constraint for scaffold-based synthetic regulatory circuits, an issue that the natural mating pathway has circumvented. Baseline leakage, however, is not a critical drawback for metabolic scaffold-based pathway, since by definition, as these pathways require an input molecule on which molecular transformations would be carried out. In addition to baseline performance, our data suggests that shifting to an optimal dose of scaffold provides only a 2-3 fold improve in signal throughput. In regulatory circuits, such quantitative changes have important implications for downstream response as we have demonstrated for pheromone-mediated cell cycle arrest. In addition, it has recently been demonstrated that even a mild change in the strength of Fus3 signaling has significant qualitative effects on the phenotypic response to pheromone stimulation (Hao et al., 2008). In other biological contexts, small differences in signals lead to drastic switch-like responses in cell decisions (Ferrell, 1996). Thus, scaffold-mediated contributions to signal flux could play a significant role in synthetic circuits. However, in metabolic circuits, improving product yield by 2-3 fold may not provide significant process advantages. Thus, our results suggest both promising opportunities and potential engineering challenges for the utilization of scaffolds in regulatory versus metabolic synthetic circuits. By quantitatively delineating these tradeoffs, our results help to define the engineering challenges that must be addressed to effectively implement scaffolds in synthetic circuits.

4. Materials and Methods

4.1 Strains

The strains used in this study are listed in Table III–1 and were kindly provided by Elaine Elion of Harvard University and by Wendell Lim of UCSF.

Table III–1. Yeast strains used in this study.

Strain	Description
CB011 ¹	W303 <i>MATa</i> , <i>ste5::KanR</i> , <i>bar1::NatR</i> , <i>far1Δ</i> , <i>mfa2::pFus1-GFP</i> , <i>his3</i> , <i>trp1</i> , <i>leu2</i> , <i>ura3</i>
EY1775 ²	W303 <i>MATa</i> , <i>ste5::TRP1</i> , <i>bar1Δ</i> , <i>his3</i> , <i>trp1</i> , <i>leu2</i> , <i>ura3</i> , <i>ade2</i> , <i>can1</i>

¹ Strain kindly provided by Wendell Lim at UCSF (Bhattacharyya et al., 2006a).

² Strain kindly provided by Elaine Elion at Harvard (Flotho et al., 2004).

4.2 Plasmid constructs

The plasmids used in this study are listed in Table III–2. Vectors containing the *STE5* allele, the *STE7* allele, the 13Myc and 3HA epitope tags, and the ADH/CYC1/GPD/TEF promoters that were kindly provided by Elaine Elion (Harvard University), Christina Smolke (Caltech), Ray Deshaies (Caltech) and David Chan (Caltech), respectively. The *STE5* allele was sub-cloned by PCR from plasmid pSKM12 (Table III–2) and was ligated into the base shuttle vector pRS416 (low-copy CEN/ARS, URA3). The *STE7* allele was sub-cloned from plasmid pVS10 (Table III–2) and was ligated into the base shuttle vector pRS415 (low-copy CEN/ARS, LEU2). The 13Myc and 3HA epitope tags were subcloned from plasmids pFA6a-13Myc-His3MX6 and pFA6a-3HA-His3MX6 (Table III–2), respectively, and were fused to the C-terminus of the gene of interest in the base shuttle vectors. The various constitutive promoters were

sub-cloned from the following vectors: p416ADH, p416CYC1, p416GPD, and p416TEF (Table III–2). The native *STE5* promoter was cloned from W303 genomic DNA by PCR, encompassing a sequence 800 bp upstream to the start codon. All promoters were inserted into the base shuttle vector immediately upstream of the start codon of the gene of interest.

Table III–2. Plasmids used in this study.

Name	Parent Vector	Promoter ¹	Description
pSC6-G	pRS416	GPD	Empty vector
pSC7-A	pRS416	ADH	STE5-13Myc ²
pSC7-C	pRS416	CYC1	STE5-13Myc
pSC7-G	pRS416	GPD	STE5-13Myc
pSC7-T	pRS416	TEF	STE5-13Myc
pSC7-P	pRS416	STE5	STE5-13Myc
pSC10-G	pRS415	GPD	Empty vector
pSC11-A	pRS415	ADH	STE7-3HA ³

¹ All promoters listed (except the native *STE5* promoter) are from (Mumberg et al., 1995).

² The *STE5* allele is from pSKM12 (Flotho et al., 2004). The 13Myc epitope tag is from pFA6a-13Myc-His3MX6 (Longtine et al., 1998).

³ The *STE7* allele is from pVS10 (van Drogen et al., 2001). The 3HA epitope tag from pFA6a-3HA-His3MX6 (Longtine et al., 1998).

4.3 Western blot

4.3-1 Cell growth and lysis

Yeast cells grown on selective media at mid-log phase growth (OD ~ 1.0, 1.3e7 cells/mL) were induced with 1.2μM α-factor or 1M sorbitol and incubated for 15 minutes at 30°C. TCA was added to 8mL cells at a final concentration of 20%, and incubated on ice for 5 minutes. Cells were then collected and washed 3x with 1mL Tris-HCl pH = 8.0 by centrifugation to ensure good solubility of protein. SDS-urea buffer [50μL water and

100 μ L of 125 mM Tris-HCl pH = 7.5, 8M urea, 4% (wt g/vol mL) SDS, 2% (vol/vol) β -mercaptoethanol, 0.02% (wt g/vol mL) bromophenol blue] was added with ~50 μ L acid-washed glass beads (425-600 μ m). Cells were homogenized using Fast Prep (Bio101 Savant) at speed 6.5 for 45 seconds, and then whole cell lysate was incubated at 42°C for 15 minutes to promote protein solubilization. After centrifugation for 15 minutes at max speed in a tabletop centrifuge, 50 μ L lysate was recovered and diluted by SDS-loading buffer [300 μ L of 50mM Tris-HCl pH = 6.8, 12% (vol/vol) glycerol, 2% (wt g/vol mL) SDS, 1% DTT, 0.01% (wt g/vol mL) bromophenol blue].

4.3-2 SDS-PAGE – quantitative Western blots only

To obtain quantitative data, many modifications to the standard Western blot protocol were made. To validate the linear comparison of samples within a gel, a standard curve consisting of ~7 data points was included with each gel as an internal control. To minimize variability of quantification, samples to be compared in a given gel were loaded in quadruplicate. Figure III-8 displays a typical quantitative Western blot for Ste5myc measurement. This approach requires the concomitant analysis of multiple samples on a single gel; thus, all quantitative gels were run using a wide-gel apparatus (TV-200YK from Topac) that accommodated 30 lanes in a single gel.

The dynamic range of the Western blot protocol is limited. To successfully detect all samples within a common dynamic range (as defined by the standard curve), samples were diluted as required in whole cell lysate of equivalent protein concentration but lacking the antigenic protein of interest. (Finding the proper dilutions for each blot was

accomplished through an iterative procedure.) We loaded lanes, whenever possible, with an equivalent lysate volume and protein concentration. This was done to mitigate pipetting error during gel loading, and to prevent horizontal band dispersion during electrophoresis (this effect complicates the box-drawing step of quantitation).

4.3-3 Immuno-blotting

Blots were transferred to nitrocellulose (Biorad) and were blocked for 1 hour in 3% milk TBST solution. Primary antibody incubation was conducted in blocking buffer overnight at 4°C. Primary antibodies and dilutions used in this study were as follows: anti-myc for detection of Ste5myc, 1:10,000 (9e10 Covance); anti-Cdc28 for equal loading control, 1:10,000 (sc-53 Santa Cruz Biotechnologies); anti-phospho-p44/42 MAPK for activity of both Fus3 and Kss1, 1:1,000 (9101 Cell Signaling Technology); anti-Fus3 for total Fus3, 1:1,000 (sc-6773 Santa Cruz Biotechnologies); anti-Kss1 for total Kss1, 1:500 (sc-28547 Santa Cruz Biotechnologies); anti-HA for detection of Ste7HA, 1:10,000 (MMS-101R Covance); and anti-phospho-p38 MAPK for phospho-Hog1, 1:1,000 (9211 Cell Signaling Technology). HRP-conjugated secondary antibodies (Biorad) were used at dilution 1:10,000. Blots were treated with Supersignal West Pico or Femto substrate (Pierce) and images were recorded using the Versa-Doc 3000 imager (Biorad).

4.3-4 Analysis – quantitative Western blots only

Signal intensities were quantified using the Volume tool in Quantity1 software. For each blot, equivalently sized, rectangular boxes were drawn around each band. A global background measurement was taken and was subtracted from all band intensities.

For each blot, a standard curve was constructed via linear regression. The signal intensities for experimental samples were averaged and then interpolated using the standard curve (Figure III-8). The interpolated values were then adjusted for the differential volumes used during loading by dividing by the respective volume loaded. The output of this calculation yields the final data from a single quantitative Western blot.

Data from anti-myc Ste5, anti-phospho-Fus3, and anti-phospho-Kss1 blots were subsequently normalized by the following equal loading controls: total Cdc28, total Fus3, and total Kss1, respectively. Signal intensities for the equal loading controls were determined through the same quantitative procedure described above.

4.4 Flow cytometry

Yeast cells grown on selective media at mid-log phase growth (OD ~ 0.1-1.0) were induced with 1.2 μ M α -factor or 1M sorbitol and incubated for 2.5 hours at 30°C. One mL ice cold TE buffer was added to 0.5mL cells. Cells were spun at 2000rcf in a tabletop centrifuge and were resuspended in 1mL cold TE buffer. Cells were briefly

vortexed to break up cell clumps, and Fus1-GFP was detected using the Cell Lab Quanta SC flow cytometer from Beckman Coulter.

Data was analyzed as described previously with the following modifications (Bhattacharyya et al., 2006a). Electronic volume, a rough measurement of cell size, was used instead of forward scatter. Cells were first gated on a side scatter versus electronic volume plot, and then cells were gated on a GFP versus side scatter plot to quantify fluorescence.

4.5 Halo assays for α -factor sensitivity

Halo assays were performed as previously described except that assays were performed on normal selective media with neutral pH (Sprague, 1991).

5. Acknowledgements

The authors thank members of the Asthagiri and Deshaies labs for helpful discussions and guidance with experiments, D. Chan, R. Deshaies, C. Smolke, E. Elion and W. Lim for reagents, and E. Davidson, R. Deshaies and P. Sternberg for comments on the manuscript. This work was supported by the Institute for Collaborative Biotechnologies through grant DAAD19-03-D-0004 from the U.S. Army Research Office. S. Chapman was supported by the NIH Molecular Cell Biology Training Grant (NIH/NRSA 5T32GM07616).

6. Supplementary Data

6.1 Quantitative Western blot analysis

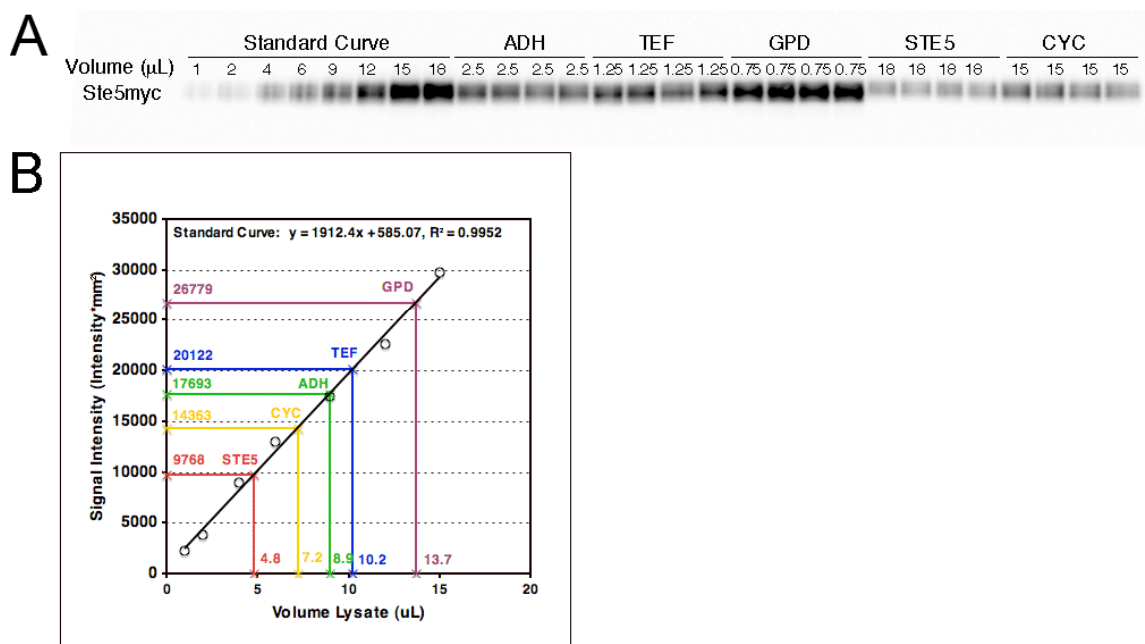


Figure III-8. Quantitative Western blot of Ste5myc abundance.

(A) Lysates of yeast expressing varying levels of Ste5myc were loaded in quadruplicate along with a standard curve in a single gel. Samples were differentially loaded by the volume indicated in order that all signals fall within the dynamic range of the standard curve. All lanes were loaded with a minimum of 15 μL total lysate using a filler lysate that lacked the antigenic protein of interest. Using Quantity1 software, boxes were drawn around the bands to obtain signal intensities (not shown). (B) Interpolation of quantitative Ste5 data from standard curve. The standard curve corresponding to the blot in part A was plotted and a linear fit was determined by regression. Mean signal intensities for the five yeast strains expressing varying amounts of Ste5 are displayed on the y-axis. The signal intensities were used to interpolate a corresponding volume of lysate from the standard curve. The interpolated values are indicated on the x-axis.

6.2 Dose-response properties as a function of *Ste5* abundance

For each expression level of *Ste5*, the dose-response data displayed in Figure III-3 and Figure III-9 were fit to the Hill equation of the following form:

$$y - y_{\min} = y_{\max} \cdot \frac{x^{n_H}}{EC50_{\alpha}^{n_H} + x^{n_H}}$$

where y is the predicted pFUS1-GFP response and x is the α -factor dose. The parameters determined by non-linear regression were y_{\min} (the pFUS1-GFP fluorescence corresponding to 0 $\mu\text{g/mL}$ pheromone), y_{\max} (the pFUS1-GFP fluorescence corresponding to 2 $\mu\text{g/mL}$), $EC50_{\alpha}$ (the dose of α -factor that elicits half-maximal response), and n_H (the Hill coefficient). Hill coefficients, $EC90_{\alpha}/EC10_{\alpha}$ (computed as $81^{1/n_H}$) and $EC50_{\alpha}$ values are listed in Table III-3.

Table III-3. Quantitative characteristics of dose-response profiles.

Promoter of <i>Ste5</i>	n_H	$EC90_{\alpha}/EC10_{\alpha}$	$EC50_{\alpha}$ (ng/mL)
STE5	0.93	110	97
CYC	1.2	40	67
ADH	1.4	26	48
TEF	1.3	30	43
GPD	1.1	46	60

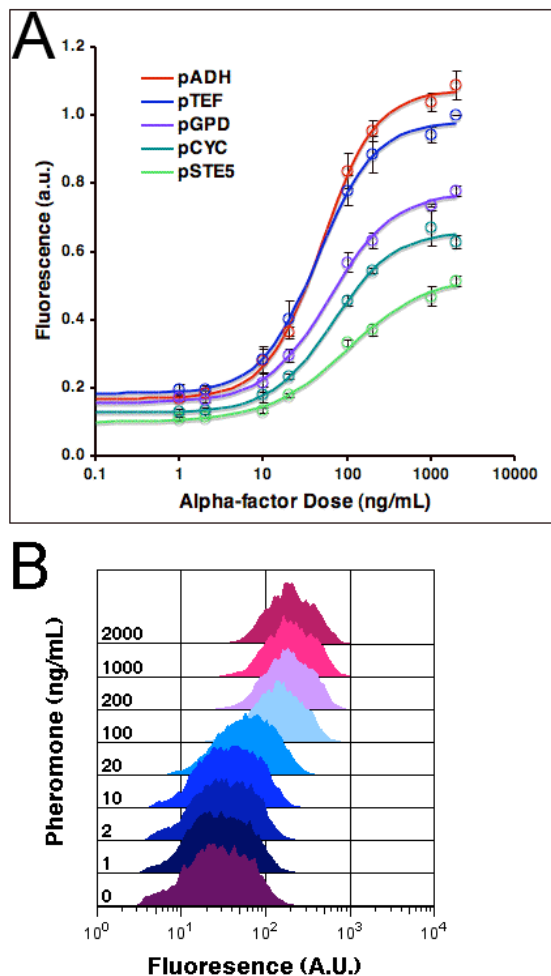


Figure III-9. Dose-response curves of pFUS1-GFP as a function of Ste5 abundance.

(A) Dose-response curves fit to Hill equation. Open circles are pFUS1-GFP data points and solid lines represent the fit to the Hill equation. Error bars on the data points denote standard error ($n=3$). See Supplementary text for more details. (B) Yeast cells expressing Ste5 from an *ADH* promoter were induced with α -factor for 2.5 h. The pFUS1-GFP reporter response was measured by flow cytometry. Histograms of GFP fluorescence are shown for various α -factor doses.

6.3 Signal fidelity is robust to perturbation in Ste5 expression

Signal crosstalk between the pheromone and high-osmolarity pathways is minimized in part through the use of two distinct scaffolds (Ste5 versus Pbs2, respectively). In addition, this scaffold-mediated fidelity is reinforced by mutual inhibition of pathway output (Figure III-10) (Bardwell, 2006; Bardwell et al., 2007; Hall et al., 1996; McClean et al., 2007; O'Rourke and Herskowitz, 1998). While mutual inhibition sharpens cell commitment to the proper response in the presence of a stimulus, our results raise the possibility that the baseline activation of Fus3/Kss1 in the absence of pheromone may inappropriately hamper the responsiveness of the high-osmolarity pathway.

To determine whether the basal activities of Fus3/Kss1 impede the high-osmolarity pathway, we measured sorbitol-mediated phosphorylation of Hog1, the high-osmolarity MAP kinase, in cells expressing different levels of Ste5. Our data show that the Hog1 signaling remains robust for all expression levels of Ste5 (Figure III-10, sorbitol). Thus, basal activation of Fus3/Kss1 does not inhibit the high-osmolarity pathway. Furthermore, this data shows that elevating Ste5 expression does not deplete the cellular pool of Ste11, allowing this upstream factor to remain available for the high-osmolarity response pathway. In fact, modulating the Ste5 expression level does not induce any inappropriate crosstalk between the pheromone and high osmolarity pathway: sorbitol treatment failed to activate pFUS1-GFP reporter above baseline levels and appropriately triggered Hog1 phosphorylation (Figure III-10). Meanwhile, pheromone stimulation did not activate Hog1, but did appropriately stimulate Fus3 and Kss1

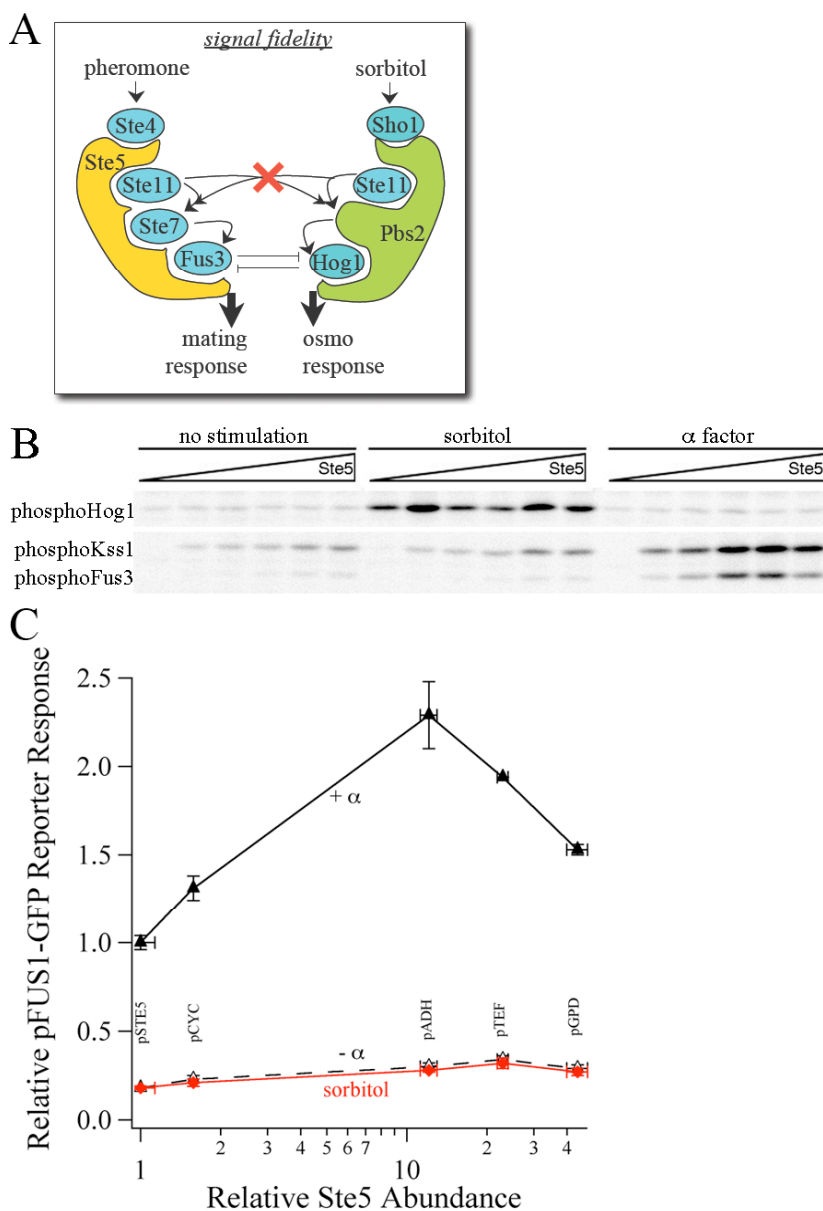
activation (Figure III-10). Thus, across nearly 50-fold change in Ste5 expression level, signal fidelity is maintained.

Figure III-10. Signal fidelity is robust to perturbations in Ste5 abundance.

(A) The fidelity of input-output response may be compromised by the presence of excess Ste5. Ste11 is a common component of the high-osmolarity pathway (right) and the mating pathway (left). Inappropriate exchange of Ste11 may cause high-osmolarity to trigger mating signals, or vice versa. Mutual inhibitory mechanisms between the two pathways prevent co-activation due to upstream leakiness.

(B) Baseline and induction of MAP kinase signaling. Yeast expressing varying levels of Ste5 were left unstimulated or stimulated with sorbitol or α -factor for 15 minutes. The phosphorylation of Hog1, Kss1, and Fus3 were monitored by Western blot. Blots are indicative of two independent trials.

(C) Baseline and induction of the mating transcriptional reporter. Yeast expressing varying levels of Ste5 were left unstimulated (gray) or stimulated with sorbitol (black) or α -factor (green) for 2.5 hours. The pFUS1-GFP reporter response was measured by flow cytometry. Error bars denote standard error (n=3).



7. *References*

- Bardwell, L. 2006. Mechanisms of MAPK signalling specificity. *Biochem Soc Trans.* 34:837-41.
- Bardwell, L., J.G. Cook, E.C. Chang, B.R. Cairns, and J. Thorner. 1996. Signaling in the yeast pheromone response pathway: specific and high-affinity interaction of the mitogen-activated protein (MAP) kinases Kss1 and Fus3 with the upstream MAP kinase kinase Ste7. *Mol Cell Biol.* 16:3637-50.
- Bardwell, L., X. Zou, Q. Nie, and N.L. Komarova. 2007. Mathematical models of specificity in cell signaling. *Biophys J.* 92:3425-41.
- Bashor, C.J., N.C. Helman, S. Yan, and W.A. Lim. 2008. Using engineered scaffold interactions to reshape MAP kinase pathway signaling dynamics. *Science.* 319:1539-43.
- Bhattacharyya, R.P., A. Remenyi, M.C. Good, C.J. Bashor, A.M. Falick, and W.A. Lim. 2006a. The Ste5 scaffold allosterically modulates signaling output of the yeast mating pathway. *Science.* 311:822-6.
- Bhattacharyya, R.P., A. Remenyi, B.J. Yeh, and W.A. Lim. 2006b. Domains, motifs, and scaffolds: the role of modular interactions in the evolution and wiring of cell signaling circuits. *Annu Rev Biochem.* 75:655-80.
- Ferrell, J.E., Jr. 1996. Tripping the switch fantastic: how a protein kinase cascade can convert graded inputs into switch-like outputs. *Trends Biochem Sci.* 21:460-6.
- Ferrell, J.E., Jr. 2000. What do scaffold proteins really do? *Sci STKE.* 2000:PE1.

- Choi, K.Y., B. Satterberg, D.M. Lyons, and E.A. Elion. 1994. Ste5 tethers multiple protein kinases in the MAP kinase cascade required for mating in *S. cerevisiae*. *Cell*. 78:499-512.
- Flotho, A., D.M. Simpson, M. Qi, and E.A. Elion. 2004. Localized feedback phosphorylation of Ste5p scaffold by associated MAPK cascade. *J Biol Chem*. 279:47391-401.
- Hall, J.P., V. Cherkasova, E. Elion, M.C. Gustin, and E. Winter. 1996. The osmoregulatory pathway represses mating pathway activity in *Saccharomyces cerevisiae*: isolation of a FUS3 mutant that is insensitive to the repression mechanism. *Mol Cell Biol*. 16:6715-23.
- Hao, N., S. Nayak, M. Behar, R.H. Shanks, M.J. Nagiec, B. Errede, J. Hasty, T.C. Elston, and H.G. Dohlman. 2008. Regulation of cell signaling dynamics by the protein kinase-scaffold Ste5. *Mol Cell*. 30:649-56.
- Kranz, J.E., B. Satterberg, and E.A. Elion. 1994. The MAP kinase Fus3 associates with and phosphorylates the upstream signaling component Ste5. *Genes Dev*. 8:313-27.
- Kusari, A.B., D.M. Molina, W. Sabbagh, Jr., C.S. Lau, and L. Bardwell. 2004. A conserved protein interaction network involving the yeast MAP kinases Fus3 and Kss1. *J Cell Biol*. 164:267-77.
- Levchenko, A., J. Bruck, and P.W. Sternberg. 2000. Scaffold proteins may biphasically affect the levels of mitogen-activated protein kinase signaling and reduce its threshold properties. *Proc Natl Acad Sci U S A*. 97:5818-23.
- Longtine, M.S., A. McKenzie, 3rd, D.J. Demarini, N.G. Shah, A. Wach, A. Brachat, P. Philippsen, and J.R. Pringle. 1998. Additional modules for versatile and

- economical PCR-based gene deletion and modification in *Saccharomyces cerevisiae*. *Yeast*. 14:953-61.
- McClellan, M.N., A. Mody, J.R. Broach, and S. Ramanathan. 2007. Cross-talk and decision making in MAP kinase pathways. *Nat Genet*. 39:409-14.
- Mumberg, D., R. Muller, and M. Funk. 1995. Yeast vectors for the controlled expression of heterologous proteins in different genetic backgrounds. *Gene*. 156:119-22.
- O'Rourke, S.M., and I. Herskowitz. 1998. The Hog1 MAPK prevents cross talk between the HOG and pheromone response MAPK pathways in *Saccharomyces cerevisiae*. *Genes Dev*. 12:2874-86.
- Park, S.H., A. Zarrinpar, and W.A. Lim. 2003. Rewiring MAP kinase pathways using alternative scaffold assembly mechanisms. *Science*. 299:1061-4.
- Pawson, T., and J.D. Scott. 1997. Signaling through scaffold, anchoring, and adaptor proteins. *Science*. 278:2075-80.
- Pryciak, P.M., and F.A. Huntress. 1998. Membrane recruitment of the kinase cascade scaffold protein Ste5 by the Gbetagamma complex underlies activation of the yeast pheromone response pathway. *Genes Dev*. 12:2684-97.
- Sprague, G. 1991. Assay of Yeast Mating Reaction. *Methods in Enzymology*. 194:77-93.
- van Drogen, F., V.M. Stucke, G. Jorritsma, and M. Peter. 2001. MAP kinase dynamics in response to pheromones in budding yeast. *Nat Cell Biol*. 3:1051-9.
- Yablonski, D., I. Marbach, and A. Levitzki. 1996. Dimerization of Ste5, a mitogen-activated protein kinase cascade scaffold protein, is required for signal transduction. *Proc Natl Acad Sci U S A*. 93:13864-9.